OPEN ACCESS
IOP Publishing
Journal of Physics: Condensed Matter
J. Phys.: Condens. Matter **37** (2025) 175802 (6pp)
https://doi.org/10.1088/1361-648X/adbece

Magnetic structure of Mn_2GaC thin film by neutron scattering

Quanzheng Tao[1,2,*], Aurelija Mockute[3], Fabio Orlandi[4], Dmitry Khalyavin[4], Pascal Manuel[4], Gunnar Palsson[5], Bachir Ouladdiaf[6], Johanna Rosen[2] and Andrew T Boothroyd[1]

[1] Department of Physics, University of Oxford, Clarendon Laboratory, Oxford OX1 3PU, United Kingdom
[2] Materials Design Division, Department of Physics, Chemistry, and Biology (IFM), Linköping University, SE-58183 Linköping, Sweden
[3] Chair for Materials Discovery and Interfaces, Institute for Materials, Faculty of Mechanical Engineering, Ruhr University Bochum, Universitätsstr. 150, 44780 Bochum, Germany
[4] ISIS Facility, STFC Rutherford Appleton Laboratory, Harwell Science and Innovation Campus, Oxfordshire OX11 0QX, United Kingdom
[5] Division of Materials Physics, Department of Physics and Astronomy, Uppsala University, Box 516, SE-75121 Uppsala, Sweden
[6] Institut Laue-Langevin, 71 avenue des Martyrs, CS 20156, 38042 Grenoble cedex 9, Grenoble, France

E-mail: quanzheng.tao@liu.se

Received 23 January 2025, revised 3 March 2025
Accepted for publication 10 March 2025
Published 21 March 2025

Abstract

MAX phases are a family of atomically laminated materials with various potential applications. Mn_2GaC is a prototype magnetic MAX phase, where complex magnetic behaviour arises due to competing interactions. We have resolved the room temperature magnetic structure of Mn_2GaC by neutron diffraction from single-crystal thin films and we propose a magnetic model for the low temperature phase. It orders in a helical structure, with a rotation angle that changes gradually between 120° and 90° depending on temperature.

Keywords: magnetic, structures, Mn_2GaC, thin, films, neutron

1. Introduction

MAX phases are based on a transition metal (M) which can be partially substituted with a rare earth, an A-group element (A), and carbon or nitrogen (X), combining the characteristics of both a metal and a ceramic [1]. MAX phases are promising materials for various applications, for example as precursors for 2D materials [2, 3]. Among them is a group of magnetic MAX phases with M = Mn, Fe, or rare earth elements [4, 5]. Here we are interested in a magnetic MAX phase thin film with M = Mn, which can potentially be used for spintronic applications [4, 6].

Mn_2GaC is a prototype magnetic MAX phase. The structure of Mn_2GaC (space group $P6_3/mmc$, no. 194) consists of Mn_2C layers interleaved with Ga layers [7, 8], see figure 1(a). The competition between antiferromagnetic and ferromagnetic interactions within the Mn_2C planes as well as between the Mn_2C planes gives rise to complex magnetic behaviours. Mn_2GaC orders magnetically below $T_N = 507$ K and shows another magnetic/structural transition at $T_C = 220$ K [9]. The second transition is accompanied by a huge contraction of the c lattice parameter [10].

The magnetic properties of Mn_2GaC have been studied extensively by first-principles calculations [11–13], from which a canted antiferromagnetic structure, with propagation vector $\mathbf{q} = (0, 0, 1/2)$ was predicted [10, 14]. Recently, a nuclear magnetic resonance study suggests a noncollinear

[*] Author to whom any correspondence should be addressed.

Original content from this work may be used under the terms of the Creative Commons Attribution 4.0 licence. Any further distribution of this work must maintain attribution to the author(s) and the title of the work, journal citation and DOI.

© 2025 The Author(s). Published by IOP Publishing Ltd

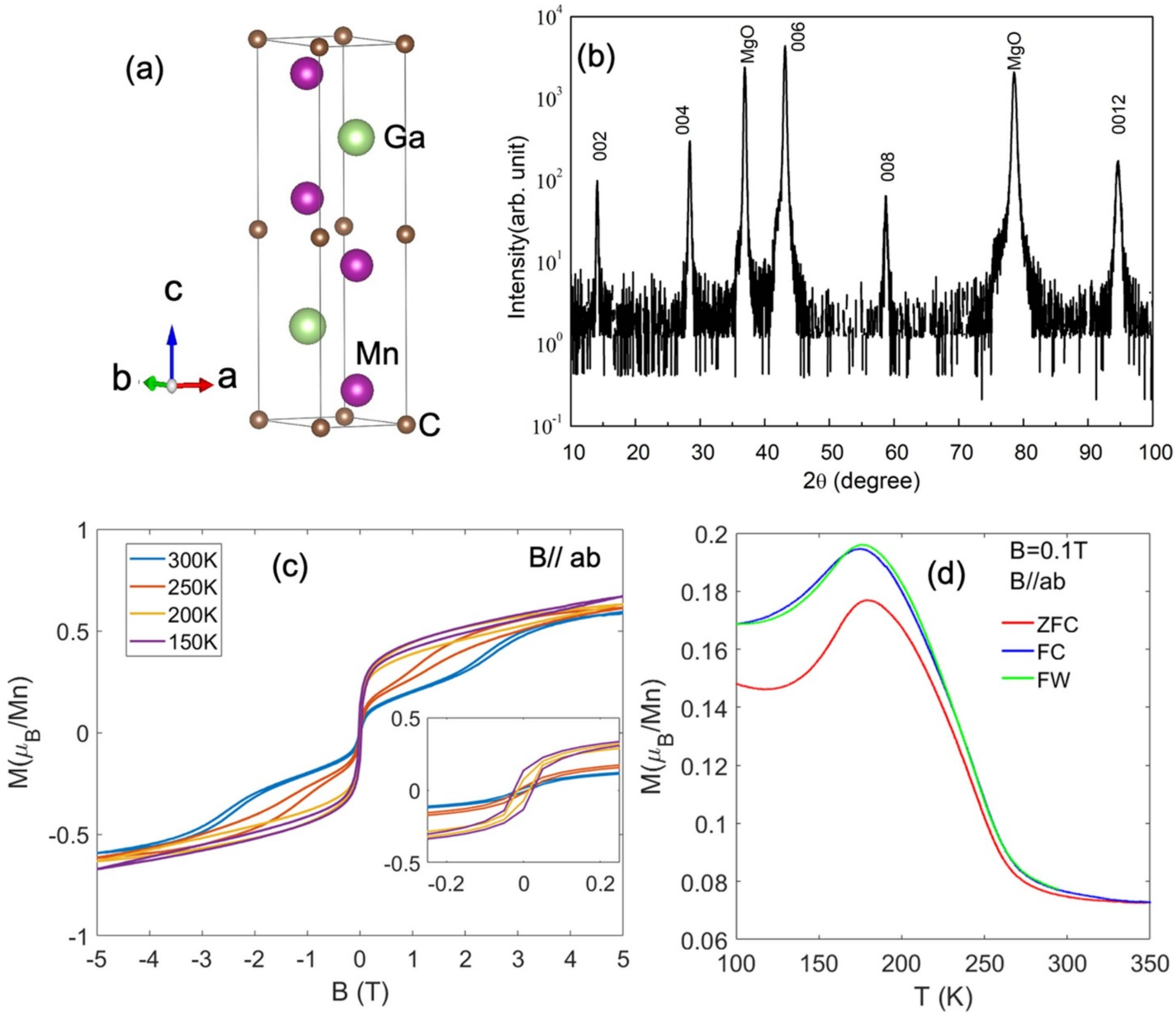

Figure 1. (a) Unit cell of Mn_2GaC. (b) X-ray θ–2θ scan a thin film of Mn_2GaC at room temperature. (c) Magnetisation vs. applied magnetic field at different temperatures. The inset shows the enlarged view of the low field region. (d) Magnetisation vs. temperature after zero-field cooling (ZFC), field cooling (FC), and field warming (FW) in a field of flux density 0.1 T.

magnetic structure and the authors speculate based on the magnetisation density that the structure may be a helical structure [15].

Mn_2GaC can only be synthesized in thin-film form, and experimental investigation of its magnetic structure have been hampered by the unavailability of bulk single crystals. Ingason *et al* studied the magnetic structure of a 50 nm thick Mn_2GaC film with neutron diffraction. They observed two magnetic reflections and proposed a structure with $\mathbf{q} = (0, 0, 1/2)$ for the low temperature structure [16]. However, due to limited Q range accessible in that experiment, the magnetic structure was not fully resolved. A slight deviation from the commensurate structure is indicated, i.e. one magnetic peak was observed at $(0, 0, L)$ with $L = 1.46$ instead of the commensurate position $L = 1.50$. Furthermore, the high temperature structure is still unknown. To better understand the complex magnetic interactions in this material, we have used neutron diffraction to study the magnetic structure over a wider Q range at both low temperature and room temperature. We find a transverse helical structure at all temperature up to T_N, with the rotation angle changing with temperature.

2. Experimental methods

Mn_2GaC thin film growth was reported previously in [7]. Briefly, thin film samples are deposited on MgO (111) single crystal substrates by magnetron sputtering from three elemental targets at 550 °C. The structural quality of the films was investigated by x-ray diffraction with a Rigaku SmartLab diffractometer. Magnetization measurements were performed with a Magnetic Properties Measurement System (Quantum Design). Neutron diffraction was performed at the time-of-flight cold neutron diffractometer WISH at the ISIS Facility [17]. The thin film sample, 150 nm Mn_2GaC on 10 mm*10 mm*0.5 mm MgO substrate, was aligned to access the $H0L$ family of reflections. The neutron beam size is 20 mm × 40 mm which is larger than the sample size, so that the whole sample is studied. The d-spacing range of WISH instrument is 0.7–50 Å. We also studied another thin film sample on the SuperAdam beamline at the Institut Laue–Langevin (ILL). The sample was measured in reflection mode.

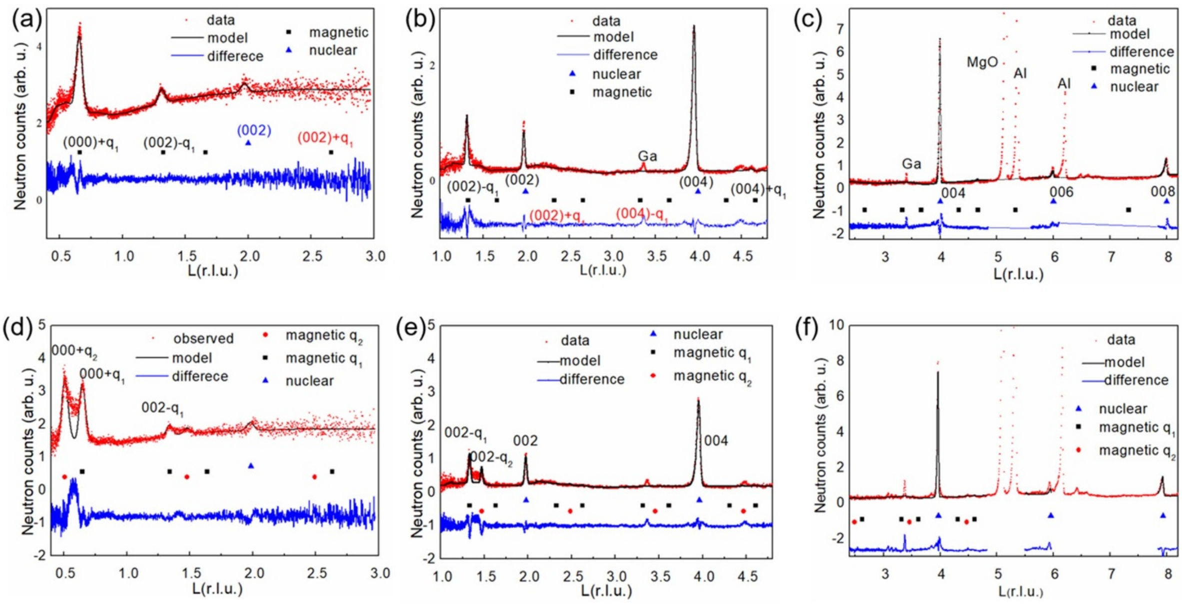

Figure 2. (a)–(c) Neutron diffraction data at 300 K along the (00*L*) direction in reciprocal space, measured at WISH at three different 2theta values (one per panel). The 00*L* reflections from Mn_2GaC are indicated with (blue) triangles. Magnetic Bragg reflections associated with $\mathbf{q}_1$ are marked with (black) squares. In (c), reflections from the MgO substrate and Al sample holder are also present. (d)–(f) Neutron diffraction at 1.5 K along the (00*L*) direction measured at WISH. Additional magnetic Bragg reflections associated with $\mathbf{q}_2$ are marked with (red) circles. The lines are calculated intensity based on the model shown in figure 3. The difference between data and model are shown (in blue) below the data.

3. Results

Figure 1(b) shows the x-ray θ–2θ scan of a 100 nm thick Mn_2GaC film on MgO substrate. Only 00*L* reflections from Mn_2GaC and MgO are present, indicating good sample quality without any impurity phase. The magnetic field (B) and temperature (T) dependent magnetisation are shown in figures 1(c) and (d). These are consistent with previous reports on Mn_2GaC [8, 9]. Briefly, at room temperature, the magnetisation shows a plateau at low field and another field-induced transition at around 2 T, while at lower temperatures it shows a weak ferromagnetic behaviour with a small hysteresis. The M vs. T curves show an increase of magnetisation below 250 K. These behaviours indicate that the magnetic structure is antiferromagnetic at room temperature, but at lower temperature it deviates from a compensated AFM structure.

Figures 2(a)–(c) shows neutron diffraction measurements of a thin film sample of Mn_2GaC at 300 K made on the WISH instrument, and figures 2(d)–(f) show the same at 1.5 K. The sample was mounted on an aluminium plate sample holder to access the *H*0*L* family of reflections. Data were collected at three rotation angles of the sample with respect to the incident neutron beam to cover a wide Q range.

At room temperature, 00*L* nuclear Bragg reflections, with $L =$ even integer, are observed as expected from the hexagonal structure. 10*L* reflections were also observed (not shown here). Figures 2(a)–(c) show the scattering intensity along the (00*L*) direction in reciprocal space. Apart from the nuclear Bragg reflections observed at $L = 2$ and $L = 4$, three additional peaks are observed at $L = 0.66$, 1.33 and 4.66. These reflections can be indexed with propagation vector $\mathbf{q}_1 = (0, 0, 0.66)$. The three reflections are indexed as (000) + $\mathbf{q}_1$, (002)$-\mathbf{q}_1$ and (004) + $\mathbf{q}_1$. It should be noted that there are no detectable peaks at (002) + $\mathbf{q}_1$ and (004)$-\mathbf{q}_1$, an observation which will be discussed later.

At 1.5 K, the 00*L* nuclear Bragg reflections with $L =$ even and the magnetic reflections from $\mathbf{q}_1$ are still present. In addition, a new set of reflections appear at low Q. These can be indexed with $\mathbf{q}_2 = (0, 0, 0.51)$. For example, the peaks at $L = 0.51$ and $L = 1.49$ can be indexed as (000) + $\mathbf{q}_2$ and (002)$-\mathbf{q}_2$. These two reflections are close to the commensurate position (0, 0, 0.5).

There is also a small peak at $L = 3.36$. This feature is identified as a powder ring in the scattering image, in contrast to the other peaks which show a well-defined spot in reciprocal space. The peak is likely from gallium metal accumulated on the surface of the film. We also attempted to search for magnetic reflections along the (10*L*) direction, but none could be observed within the resolution of the WISH instrument, most likely due to their small structure factors and the non-negligible mosaic spread.

Representation analysis is performed with the BasIreps program which is part of Fullprof suite [18]. For the space group P63/mmc (no. 194) with $\mathbf{q} = (0, 0, \delta)$ and Mn in the 4*f* Wyckoff position, the magnetic decomposition is characterized by 2 one-dimensional irreducible representations (Irreps) and 2 two-dimensional irreducible representations: $\Gamma_{mag} = mDT_2 + mDT_3 + mDT_5 + mDT_6$.

The one-dimensional Irreps mDT_2 and mDT_5 corresponds to structures with moment aligned along the c axis. They can be excluded because if the moments are along c then the 00*L* magnetic reflections would have zero intensity in neutron diffraction, contrary to what is observed.

Table 1. Summary of the refined crystal and magnetic structure parameters of Mn_2GaC at temperatures of 300 K and 1.5 K.

	300 K	1.5 K	
Mn(1/3, 2/3, z)	$z = 0.586(1)$	0.579(1)	
c (Å)	12.56(1)	12.54(1)	
Propagation vector	$\mathbf{q}_1 = (0, 0, 0.667(3))$	$\mathbf{q}_1 = (0, 0, 0.656(1))$	$\mathbf{q}_2 = (0, 0, 0.512(1))$
Mn moment (μ_B)	1.51(5)	1.28(3)	1.09(3)

mDT_3 corresponds to a helical structure with rotation angle $\theta = \pi\delta/2$, which leads to reflections at $002 + \mathbf{q}$ position and $004–\mathbf{q}$ but no observable reflections at $000 + \mathbf{q}$ and $002-\mathbf{q}$, contrary to the experimental observation. mDT_6 agrees well with experimental diffraction pattern. mDT_6 corresponds to helical structure with rotation angle $\theta = \pi\delta$. In this structure the relative intensities of the $00L$ magnetic reflections are given by

$$I(00L) = f^2(Q)\cos^2(\pi dL)\{6 - 2\cos(\pi L) - 4\cos(2\pi L)\},$$

where $f^2(Q)$ is the squared magnetic form factor of Mn, and $d = 2z–1 \approx 1/6$. For $\mathbf{q} = \mathbf{q}_1 = (0, 0, 2/3)$, the intensities of the $002 + \mathbf{q}_1$ and $004-\mathbf{q}_1$ reflections are seen to be about 20 times smaller than the $000 + \mathbf{q}_1$ and $002-\mathbf{q}_1$ reflections.

After narrowing the candidate structures, we performed refinement of the $00L$ scattering pattern. We first refined the crystal structure with the $00L$ nuclear reflections. Owing to the negative scattering length of Mn, the structure factors of the $00L$ reflections are especially sensitive to the position of Mn. We could refine the c lattice parameter and z height parameter for Mn on the $4f$ site (1/3, 2/3, z). It is worth mentioning that the position of Ga and C are fixed by symmetry. Although the $10L$ reflections are clearly observable, they are broader than the $00L$ reflections, which makes a quantitative analysis difficult. This simplified approach is justified as we performed the crystal structure refinement only for the scale factor for calculating the magnetic moment size. For our purpose, the obtained information from $00L$ is sufficient, so we only include these reflections in the structural refinement. We refined the magnetic moment and found a value of $1.51(5)\mu_B$/Mn at room temperature. The refined structural and magnetic parameters are summarised in table 1.

Now we turn to the temperature dependence of the magnetic structure. After establishing the $\mathbf{q}_1 = (0, 0, 2/3)$ structure, we could extend the analysis to any $\mathbf{q}$ vector of the form of $\mathbf{q} = (0, 0, \delta)$. The symmetry consideration is the same for $\mathbf{q} = (0\ 0\ \delta)$, when δ is not 0 or 1/2. At 1.5 K, the magnetic reflections can be indexed with $\mathbf{q}_1 = (0, 0, \sim 2/3)$ and $\mathbf{q}_2 = (0, 0, 0.51)$. Like the analysis on the 120° structure, the $\mathbf{q}_2$ structure can be described by a transverse helix but with a different rotation angle. The rotation angle can be calculated based on the propagation vector, $\theta = \pi\delta$. For $\mathbf{q}_1 = (0, 0, 2/3)$, $\theta = 120°$ as before, while for $\mathbf{q}_2 = (0, 0, 0.51)$, $\theta = 92°$. A schematic of the $\mathbf{q}_2$ structure is shown in figure 3(b).

The evolution of the $(002) + \mathbf{q}$ peaks was also studied at elevated temperatures up to T_N on a different thin film sample at the SuperAdam instrument, as shown in figure 4. The $\mathbf{q}_1$ and $\mathbf{q}_2$ peaks coexist near room temperature, but with increasing temperature the intensity of the $\mathbf{q}_2$ peak decreases quickly (the red curve) and the position of the $\mathbf{q}_1$ peak shifts towards $L = 0.5$. Accordingly, the δ value is changing between 0.48–0.63. On cooling below T_N, therefore, the rotation angle of the dominant $\mathbf{q}_1$ phase changes from about 86° to 120°. At around 500 K, close to T_N, the magnetic intensity is no longer detectable.

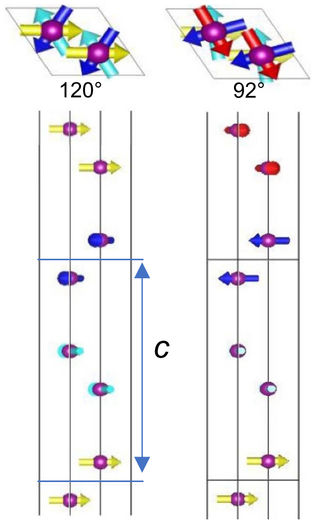

Figure 3. Magnetic structures of thin film Mn_2GaC at room temperature (left) and at 1.5 K (right). For clarity, only Mn atoms are shown in the schematic. At room temperature, the spins in each Mn_2C layer rotate 120° across the Ga layer. At 1.5 K, the angle is 92°. The size of crystallographic unit cell in the interlayer direction is indicated by the arrow.

4. Discussion

The determination of magnetic structures by neutron diffraction from thin-film samples is challenging because of the small volume of material. We have obtained a solution for the room temperature structure $\mathbf{q}_1$ based on a small number of detected reflections. The structure comprises a 120° transverse helix formed from pairs of ferromagnetically aligned nearest-neighbour Mn spins. Below room temperature, a second propagation vector $\mathbf{q}_2$ is observed which coexists with $\mathbf{q}_1$. The $\mathbf{q}_2$ component is similar to the $\mathbf{q}_1$ but has a rotation angle of $\sim$90° instead of 120°. The limitations of our data prevent us from saying whether $\mathbf{q}_1$ and $\mathbf{q}_2$ represent two spatially distinct magnetic phases, or whether it is a uniform phase whose magnetic structure has two Fourier components.

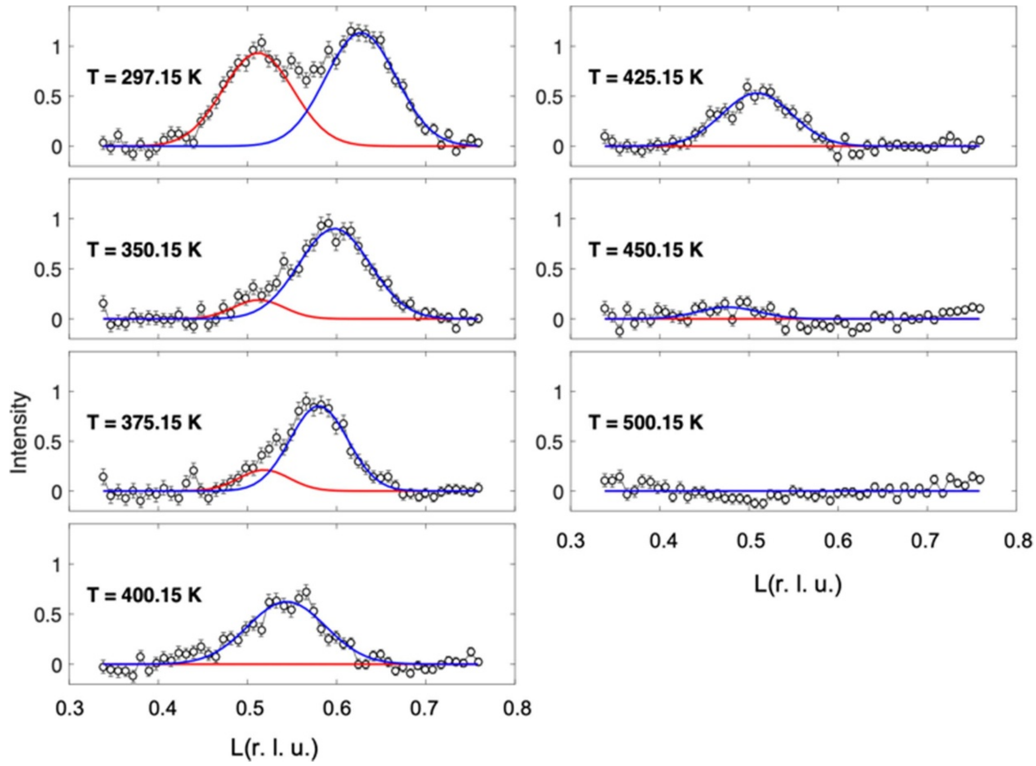

Figure 4. Temperature evolution of (0, 0, 0)+ **q** peaks from room temperature to above T_N, measured at SuperAdam. The blue and red lines are fits to the $\mathbf{q}_1$ and $\mathbf{q}_2$ peaks, respectively.

From our previous study, we know that a structural distortion takes place at $T_c = 220$ K, below which the c lattice parameter shrinks by as large as 0.2% [10]. However, the exact nature of the structural change is not known. A determination of the low temperature crystal structure could lead to a more accurate magnetic structure for the low temperature phase, which would be a topic for future study. Another remaining question is the appearance of a weak ferromagnetic moment in the *a–b* plane starting below ∼250 K, as observed in the bulk magnetisation, figure 1(d). Our proposed helical structure works for the room temperature phase which has no net magnetic moment. But the helical structure proposed in this work cannot account for the net moment in the low temperature phase either if the two Fourier components are considered together or as two different magnetic phases. Most likely, the weak moment comes from canting in the *a–b* plane, as suggested in [10]. The canting would result in an additional propagation vector, **q** = (0 0 0), which means a small magnetic contribution to the structural allowed reflections for example (002). However, the magnetic signal from a small, canted moment on top of the strong nuclear reflections, e.g. (002), is not within the sensitivity of the current experiment.

Helical structures are found in many rare earth based magnetic materials, for example elemental Tb and Ho, and rare earth compounds, e.g. EuCuAs [19, 20]. For these hexagonal materials, the Dzyaloshinskii–Moriya interaction is not expected, and the helical structures are usually considered to be the result of competing interactions. In the present material, the RKKY interaction is also expected to be a factor, considering its metallic nature [21]. Thus, one possibility is that the nearest-neighbour interaction is ferromagnetic, forming ferromagnetic pairs in the Mn_2C plane, but that it changes sign as a function of distance along *c*-axis. The evolution of the rotation angle as a function of temperature may reflect the delicate balance of the competing interactions. It would be interesting to study the structure in the presence of external stimuli such as applied pressure or magnetic field. Chemical doping would also be expected to tune the magnetic structure.

Our experimentally obtained magnetic structure of Mn_2GaC will help with the understanding of the wider family of magnetic MAX phases. Most of the previous *ab initio* theoretical studies have only considered simple collinear magnetic structures. Our results suggest that more complex noncollinear and/or incommensurate structure should be considered as well. Although incommensurate structures with large magnetic unit cell would be too demanding for calculation, the two simple cases with rotation angle of 90° and 120°, which are close to what is observed in Mn_2GaC, may be amenable to calculation by *ab initio* methods.

5. Conclusion

We have investigated the magnetic structure in a thin film of Mn_2GaC in the full temperature range by neutron diffraction. It orders below $T_N = 507$ K in a transverse helical structure. The rotation angle of the helix changes with temperature on cooling to room temperature. Below room temperature a second transverse helix emerges with a different rotation angle. The observed magnetic structures differ from those previously considered in *ab initio* calculations, which emphasises the importance of determining magnetic structures experimentally for the understanding of magnetic MAX phases. The determination of the magnetic structures in a thin film of Mn_2GaC was possible thanks to improvements in neutron diffraction instrumentation, and the techniques used here could also be applied to solve magnetic structures in other magnetic thin films.

Data availability statement

All data that support the findings of this study are included within the article (and any supplementary files).

Acknowledgment

Q T acknowledges support from the Swedish Research Council Grant No. 2021-00471. A M acknowledges the Swedish Research Council Grant No. 2015-00607 Experiments at the ISIS Neutron and Muon Source were supported by a beamtime allocation RB2220353 from the Science and Technology Facilities Council. Data is available here: 10.5286/ISIS.E.RB2220353-1. Data obtained from ILL is available here doi:10.5291/ILL-DATA.5-54-325.

ORCID iDs

Quanzheng Tao https://orcid.org/0000-0002-4073-5242
Fabio Orlandi https://orcid.org/0000-0001-6333-521X
Gunnar Palsson https://orcid.org/0000-0001-5997-8597

References

[1] Sokol M, Natu V, Kota S and Barsoum M W 2019 *Trends Chem.* **1** 210
[2] Naguib M, Kurtoglu M, Presser V, Lu J, Niu J, Heon M, Hultman L, Gogotsi Y and Barsoum M W 2011 *Adv. Mater.* **23** 4248
[3] VahidMohammadi A, Rosen J and Gogotsi Y 2021 *Science* **372** eabf1581
[4] Ingason A S *et al* 2013 *Phys. Rev. Lett.* **110** 195502
[5] Tao Q *et al* 2019 *Chem. Mater.* **31** 2476
[6] Ingason A S, Dahlqvist M and Rosén J 2016 *J. Phys.: Condens. Matter* **28** 433003
[7] Ingason A S *et al* 2014 *Mater. Res. Lett.* **2** 89
[8] Thorsteinsson E B, Ingason A S and Magnus F 2023 *Phys. Rev. Mater.* **7** 034409
[9] Novoselova I P *et al* 2018 *Sci. Rep.* **8** 2637
[10] Dahlqvist M *et al* 2016 *Phys. Rev.* B **93** 014410
[11] Dahlqvist M and Rosen J 2020 *Sci. Rep.* **10** 11384
[12] Thore A, Dahlqvist M, Alling B and Rosén J 2014 *J. Appl. Phys.* **116** 103511
[13] Thore A, Dahlqvist M, Alling B and Rosén J 2016 *Phys. Rev.* B **93** 054432
[14] Jönsson H, Ekholm M, Leonov I, Dahlqvist M, Rosén J and Abrikosov I 2022 *Phys. Rev.* B **105** 035125
[15] Dey J, Jedryka E, Kalvig R, Wiedwald U, Farle M, Rosen J and Wójcik M 2023 *Phys. Rev.* B **108** 054413
[16] Ingason A S, Pálsson G K, Dahlqvist M and Rosén J 2016 *Phys. Rev.* B **94** 024416
[17] Chapon L C *et al* 2011 *Neutron News* **22** 22
[18] Rodríguez-Carvajal J 1993 *Physica* B **192** 55
[19] Blundell S 2001 *Magnetism in condensed matter* (OUP Oxford)
[20] Soh J-R *et al* 2023 Weyl metallic state induced by helical magnetic order (arXiv:2305.00295 2023)
[21] Ruderman M A and Kittel C 1954 *Phys. Rev.* **96** 99